ADVANCED MATERIALS

ing the processed template into contact with a 2 cm × 2 cm silicon wafer piece (with native oxide) or a gold-coated silicon wafer piece, placed on a hot plate and heated to 120 °C in both cases. The PDMS template was pressed slightly onto the substrate until conformal contact was visibly established. Immediately after contact was achieved, the template and substrate were removed from the hot plate, allowed to cool down, and then separated.

Received: June 07, 2005
Final version: July 25, 2005
Published online: September 5, 2005

[1] F. Caruso, *Colloids and Colloidal Assemblies*, Wiley-VCH, Weinheim, Germany **2004**.
[2] W. Caseri, *Macromol. Rapid Commun.* **2000**, *21*, 705.
[3] A. Bell, *Science* **2003**, *299*, 1688.
[4] P. K. Mallick, *Fiber-Reinforced Composites: Materials, Manufacturing, and Design*, Dekker, New York **1993**.
[5] C. Murray, C. Kagan, M. Bawendi, *Annu. Rev. Mater. Sci.* **2000**, *30*, 545.
[6] T. Trindade, P. O'Brien, N. L. Pickett, *Chem. Mater.* **2001**, *13*, 3843.
[7] C. Lopez, *Adv. Mater.* **2003**, *15*, 1679.
[8] F. Garcia-Santamaria, H. T. Miyazaki, A. Urquila, M. Ibisate, M. Belmonte, N. Shinya, F. Meseguer, C. Lopez, *Adv. Mater.* **2002**, *14*, 1144.
[9] S. Maenosono, T. Okubo, Y. Yamaguchi, *J. Nanopart. Res.* **2003**, *5*, 5.
[10] G. Whitesides, M. Boncheva, *Proc. Natl. Acad. Sci.* **2002**, *99*, 4769.
[11] H. O. Jacobs, A. R. Tao, A. Schwartz, D. H. Gracias, G. M. Whitesides, *Science* **2002**, *296*, 323.
[12] X. R. Xiong, Y. Hanein, J. D. Fang, Y. B. Wang, W. H. Wang, D. T. Schwartz, K. F. Böhringer, *J. Microelectromech. Sys.* **2003**, *12*, 117.
[13] H.-J. J. Yeh, J. S. Smith, *IEEE Photonics Technol. Lett.* **1994**, *6*, 706.
[14] Y. Xia, Y. Yin, Y. Lu, J. McLellan, *Adv. Funct. Mater.* **2003**, *13*, 907.
[15] N. D. Denkov, O. D. Velev, P. A. Kralchevsky, O. B. Ivanov, H. Yoshimura, K. Nagayama, *Nature* **1993**, *361*, 26.
[16] J. Cecil, D. Vasquez, D. Powell, *Int. J. Prod. Res.* **2005**, *43*, 819.
[17] U. Srinivasan, M. Houston, R. Howe, R. Maboudian, *J. Microelectromech. Sys.* **1998**, *7*, 252.
[18] S. Hur, D. Khang, C. Kocabas, J. Rogers, *Appl. Phys. Lett.* **2004**, *85*, 5730.
[19] K. L. Johnson, K. Kendall, A. D. Roberts, *Proc. R. Soc. Lond. A* **1971**, *324*, 301.
[20] J. J. Bikerman, *The Science of Adhesive Joints,* Academic Press, New York **1968**.
[21] A. Bietsch, B. Michel, *J. Appl. Phys.* **2000**, *88*, 4310.
[22] C. Drummond, D. Chan, *Langmuir* **1997**, *13*, 3890.
[23] Y. Sun, D.-Y. Khang, F. Hua, K. Hurley, R. G. Nuzzo, J. A. Rogers, *Adv. Funct. Mater.* **2005**, *15*, 30.
[24] H. Schmid, H. Wolf, R. Allenspach, H. Riel, S. Karg, B. Michel, E. Delamarche, *Adv. Funct. Mater.* **2003**, *13*, 145.
[25] K. Gilleo, *Area Array Packaging Handbook: Manufacturing and Assembly*, McGraw-Hill Professional, New York **2001**.
[26] Y. Cui, M. T. Björk, J. A. Liddle, C. Sönnichsen, B. Boussert, A. P. Alivisatos, *Nano Lett.* **2004**, *4*, 1093.
[27] A. Bernard, D. Fitzli, P. Sonderegger, E. Delamarche, B. Michel, H. R. Bosshard, H. Biebuyck, *Nat. Biotechnol.* **2001**, *19*, 866.
[28] V. Santhanam, R. P. Andres, *Nano Lett.* **2004**, *4*, 41.
[29] D. L. Klein, R. Roth, A. K. L. Lim, A. P. Alivisatos, P. L. McEuen, *Nature* **1997**, *389*, 699.
[30] S. Kolliopoulou, P. Dimitrakis, P. Normand, H. L. Zhang, N. Cant, S. D. Evans, S. Paul, C. Pearson, A. Molloy, M. C. Petty, D. Tsoukalas, *J. Appl. Phys.* **2003**, *94*, 5234.
[31] A. B. Kharitonov, A. N. Shipway, I. Willner, *Anal. Chem.* **1999**, *71*, 5441.
[32] M. Geissler, H. Wolf, R. Stutz, E. Delamarche, U. W. Grummt, B. Michel, A. Bietsch, *Langmuir* **2003**, *19*, 6301.

Thin Films of Block Copolymers as Planar Optical Waveguides**

By *Dong Ha Kim*,* *King Hang Aaron Lau*, *Joseph W. F. Robertson*, *Ok-Joo Lee*, *Unyong Jeong*, *Jeong In Lee*, *Craig J. Hawker*, *Thomas P. Russell*, *Jin Kon Kim*, and *Wolfgang Knoll**

Block copolymers (BCPs) have attracted significant attention as nanostructured materials, since they self-assemble to form well-defined, ordered, periodic nanoscale morphologies depending on the relative volume fraction of the constituent blocks.[1,2] The versatility of this unique class of polymers offers tremendous potential for their use as templates and scaffolds for applications in microelectronics, separation devices, optics, and optoelectronics.[3–8] While polymer-based optical-waveguide materials have been widely discussed,[9] little attention has been paid to BCP systems[10] in regard to their applications in the field of optical elements. Since the domain size and chemical nature of BCPs can be tailored by controlling the molecular weight and by incorporating specific functionality, BCPs may be ideal candidates for waveguide materials with tunable periodic dielectric constants and optimized physicochemical properties in integrated optical devices. Here, we demonstrate that thin films of BCPs with controlled microdomain orientation can be employed as planar optical waveguides and we investigate their waveguiding properties by optical waveguide spectroscopy (OWS).[11–13]

Resonance coupling between surface plasmons (or plasmon surface polaritons) and incident photons can occur at a metal/dielectric interface, especially in the experimental setup

[*] Dr. D. H. Kim, Prof. W. Knoll, K. H. A. Lau, Dr. J. W. F. Robertson, Dr. O.- J. Lee
Max Planck Institute for Polymer Research
Ackermannweg 10, D-55128 Mainz (Germany)
E-mail: kimdh@mpip-mainz.mpg.de; knoll@mpip-mainz.mpg.de
Dr. U. Jeong,[+] J. I. Lee, Prof. J. K. Kim
National Creative Research Initiative Center for
Block Copolymer Self-Assembly
Department of Chemical Engineering
and Polymer Research Institute
Pohang University of Science and Technology
Hyoja-dong, San 31, Nam-gu, Pohang, Kyungbuk 790–784 (Korea)
Prof. C. J. Hawker
Department of Chemistry
University of California at Santa Barbara
Santa Barbara, CA 93106 (USA)
Prof. T. P. Russell
Silvio O. Conte National Center for Polymer Research
Polymer Science and Engineering Department
University of Massachusetts at Amherst, Amherst, MA 01003 (USA)
[+] Current Address: Department of Chemistry, University of Washington, Seattle, WA 98195–1700, USA.

[**] The authors are grateful for financial support by the Deutsche Forschungsgemeinschaft (DFG) in the frame of priority program, Schwerpunktprogramm 1165 (SPP 1165: KN 224/15–1). J. K. Kim acknowledges the support of the Creative Research Initiative Program by the Korea Science and Engineering Foundation (KOSEF).

  DOI: 10.1002/adma.200500170

known as the Kretschmann configuration (Fig. 1).[11,12,14,15] If the thickness of the dielectric layer is further increased (in organic polymeric layers typically thicker than ~200 nm), waveguide optical modes, in addition to surface plasmon resonance,

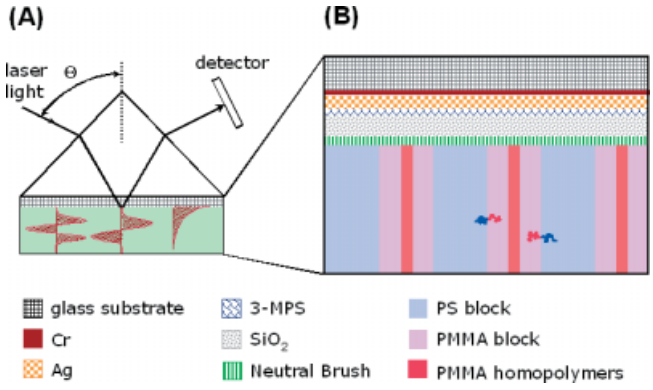

Figure 1. A) Schematic diagram of the OWS setup based on the Kretschmann configuration, and of the idealized field distributions of several guided modes in the waveguiding layer. B) Schematic diagram of a thin film of PS-*b*-PMMA/PMMA homopolymer mixture with PMMA microdomains aligned normal to the substrate surface fabricated onto glass substrate (LaSFN9 glass/Cr/Ag/3-MPS/SiO_2/PS-*r*-PMMA/BCP/air). PS: polystyrene; PMMA: poly(methyl methacrylate); 3-MPS: 3-mercaptopropyl trimethoxysilane.

can be observed.[11,12,15] In this communication, thin films of mixtures of polystyrene-*block*-poly(methyl methacrylate) (PS-*b*-PMMA) and PMMA homopolymers with the cylindrical PMMA microdomains oriented normal to the film plane were used to couple waveguide optical modes, and typical nanofabrication processes occurring inside the layer were monitored by OWS. Here, the confinement of the PMMA homopolymer to the microdomains markedly enhances the aspect ratio of the microdomain orientation by ~10 times the bulk period (L_0),[16] which makes the film appropriate as model BCP waveguide layers.

The PS-*b*-PMMA/PMMA thin films were combined in the Kretschmann prism coupling geometry as schematically depicted in Figures 1A,B. Thin chromium (~2.6 nm) and silver (~43.6 nm) coupling gap layers were successively deposited on glass substrates attached to the coupling prism with an index-matching oil. The glass prism and substrate thus form an optically continuous medium. The BCP thin films were deposited and ordered on the glass substrate (described below), with several coupling layers in between (Fig. 1B), before the substrate was mounted onto the prism base.

A self-assembled monolayer of ~2.2 nm thick 3-mercaptopropyl trimethoxysilane (3-MPS) was adsorbed onto the evaporated Ag layer to promote adhesion between the Ag and the silicon dioxide (SiO_2) layer. The Ag substrate was immersed in 20 mM 3-MPS in dry ethanol for 2 h. The surfaces were then rinsed with copious amounts of dry ethanol and deionized (Milli-Q) water. Hydrolysis and condensation of the 3-MPS layers was performed in 0.1 M HCl for 1 h. The Ag surfaces were removed from the HCl solution after 3-MPS condensation steps and rinsed with water. SiO_2 layers were prepared by a sol–gel process according to a method reported previously.[17,18] The hydrolyzed solution of the sol–gel precursors was delivered onto the 3-MPS-modified Ag surface, and the sample was spun at ~3400 rpm for 1 min, producing films with a thickness of ~33.1 nm. The Ag/3-MPS/SiO_2 surface was stored in a desiccator at room temperature for a minimum of 2 days to complete the condensation process, and to remove any residual solvent.

An energetically neutral surface for PS-*b*-PMMA films was prepared on the SiO_2 layer using a hydroxy terminated poly(styrene-*co*-methyl methacrylate) random copolymer (PS-*r*-PMMA) via the covalent coupling between the hydroxyl groups and the SiO_2 surface.[19,20] PS-*r*-PMMA was anchored to the SiO_2 surface by spin-coating a 2 wt.-% toluene solution at 1000 rpm, followed by annealing under vacuum at 165 °C for 3 days. After rinsing with toluene a well-defined, thin layer of PS-*r*-PMMA with a thickness of ~4.2 nm remained.

Thin films composed of PS-*b*-PMMA and PMMA homopolymer mixture, containing 25 wt.-% PMMA homopolymers with respect to the amount of PMMA block, were prepared by spin-coating 5 wt.-% toluene solutions at 1000 rpm onto the PS-*r*-PMMA surface. The films were annealed at 155 °C for 2 days under vacuum, and then quenched to room temperature. Figure 2A illustrates the phase contrast atomic force microscopy (AFM) image of the surface of a PS-*b*-PMMA/PMMA film deposited onto a glass substrate as schematically shown in Figure 1B. The darker and brighter areas are PS matrix and PMMA microdomains, respectively. Hexagonally packed arrays of cylindrical PMMA microdomains oriented normal to the substrate are seen over a wide area of the film. The average center-to-center distance (λ_{C-C}) between PMMA microdomains was ~46 nm. Deep UV exposure of the films, followed by acetic acid rinsing, was used to selectively remove PMMA microdomains and produce an ordered, nanoporous template. Figure 2B shows a height contrast AFM image of

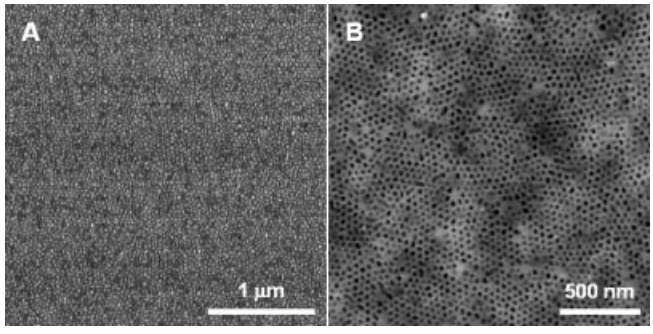

Figure 2. A) Phase contrast AFM image of the surface of PS-*b*-PMMA/PMMA film. The image shows an area of 3 μm × 3 μm. B) Height contrast AFM image of the surface of the identical film in (A) after PMMA microdomains were removed by UV exposure and acetic acid rinsing. The image shows a 2 μm × 2 μm area on the surface.

ADVANCED MATERIALS

the arrays of nanopores (darker areas) in a crosslinked PS matrix after removal of the PMMA microdomains.

The waveguide patterns of the initial BCP film (blue full curves) are displayed in Figures 3A,B for s- and p-polarization, respectively, where characteristic transverse electric (TE) and transverse magnetic (TM) modes are observed. The best fits (blue dotted curves) to the experimental curves were obtained from Fresnel calculations to give the dielectric constants (ε) and film thicknesses (h), respectively.

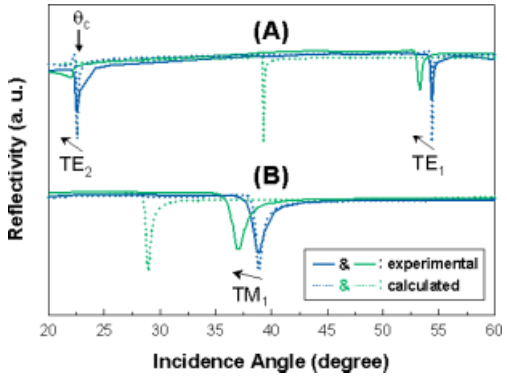

Figure 3. Waveguide mode patterns of the initial BCP film and the porous PS template by OWS along with the simulated curves in s-polarization (A) and in p-polarization (B), respectively. The blue and green curves represent the waveguide patterns for the original films and those after the removal of PMMA microdomains, respectively. The blue dotted curves are the best fits to the waveguide patterns of the initial film. The green dotted curves are hypothetical patterns obtained from the Fresnel calculation using values derived from Equations 1,2, assuming that all PMMA microdomains were completely removed by UV exposure and acetic acid rinsing (a_S value of 2.58 was used for this crosslinked PS matrix). Best fits to the waveguide patterns of the porous PS template were not included. Shifts of the resonance coupling modes due to pore generation are indicated by arrows.

Broadening of the coupling dip and the decrease in amplitude of the experimental data compared with the calculated curves is attributed to the distribution in pore diameter and to the surface roughness of the film, which may disrupt the spatial coherence in the waveguide coupling conditions across the measured areas (~1 mm^2), corresponding to the laser-beam size. The guided coupling modes of the BCP layer are entirely dictated by its effective dielectric constant (ε_{eff}) and its film thickness. The symmetry of the microdomain morphology: an array of cylinders with the axis aligned normal to the substrate surface dictates that one of the principal axes of the dielectric function, $\varepsilon_{eff}=\{\varepsilon_x, \varepsilon_y, \varepsilon_z\}$, is parallel to the cylinder axis and that the two other axes are parallel to the film surface. As shown in Figure 2A, the distribution of the cylindrical domains is isotropic, so we assume $\varepsilon_x=\varepsilon_y$. Therefore, three parameters, $\varepsilon_x(=\varepsilon_y)$, ε_z, and h need to be determined from the s- and p-polarized waveguide mode spectra.

The dielectric constants and the film thicknesses, obtained from fitting the experimental data in Figure 3 and using the Fresnel calculation, are as follows: $\varepsilon_x=\varepsilon_y=2.402$, $\varepsilon_z=2.429$, and $h=349$ nm.[11] The thicknesses of the underlying layers (Cr, Ag, 3-MPS, SiO_2, and PS-*r*-PMMA) were determined separately by surface plasmon resonance (SPR) spectroscopy with the refractive indexes of the 3-MPS, SiO_2, and PS-*r*-PMMA layers being 1.444, 1.460, and 1.549, respectively.

The pore generation by UV and acetic acid etching was detected via shifts of the mode coupling angles to lower values (indicated by arrows) due to a decrease in ε_{eff} (note that $\varepsilon_{air}=1.0$ is much lower than $\varepsilon_{PMMA}=2.22$), as shown in Figure 3 (green full curves). The degree of shift ($\Delta\theta$) for the TM_1 mode was measured to be 1.9° (from $\theta=38.9°$ to $\theta=37.0°$) and that for the TE_1 mode was 1.1° (from $\theta=54.4°$ to $\theta=53.3°$). The TM_2 mode was, however, convoluted with the critical angle (θ_c) due to total internal reflection, and is not used for the analysis. Fresnel fitting (curves not shown) gives $\varepsilon_x=\varepsilon_y=2.377$, $\varepsilon_z=2.385$, and $h=341$ nm, for the porous template. From the decrease in the refractive index compared with the initial film, it is evident that sections of the PMMA chains were removed. For comparison, the optical constants (Ψ and Δ) of the films were measured by variable angle spectroscopic ellipsometry (VASE; J. A. Woollam Co., Inc.) at an incidence angle of 70° and best fit to the experimental data using Wvase32 software. The effective dielectric constants of the initial BCP film and the porous template were calculated to be ~2.40 and 1.85, respectively.

ε values can also be calculated from the effective medium theory, suitable for the present case, where the domain size is much smaller than the wavelength of guided light, using the following equations[21,22]

$$\varepsilon_x = \varepsilon_y = \varepsilon_S + \frac{\varepsilon_S f_D(\varepsilon_D - \varepsilon_S)\beta}{\varepsilon_S - 1/2 f_D(\varepsilon_D - \varepsilon_S)\beta} \quad (1)$$

$$\varepsilon_z = f_D\varepsilon_D + f_S\varepsilon_S \quad (2)$$

where f is the volume fraction,

$$\beta = 2\frac{\varepsilon_S}{\varepsilon_D + \varepsilon_S} \quad (3)$$

and D and S represent cylindrical domain initially occupied by PMMA and PS matrix, respectively. ε_{PMMA} and ε_S values used in this study were 2.22 and 2.53, respectively, for the initial BCP film. The ε_S value of the crosslinked PS after UV exposure was ~2.58 measured by VASE and used for the prediction of the PS template.

The predicted patterns (green dotted curves) thus obtained, with the assumption that the PMMA microdomains were removed completely, are also shown in Figure 3. It was found that the coupling angles appear at lower angles than those of the experimentally observed patterns (green full curves), indicating that sections of the PMMA chains still remain after the etching condition used in this study. Comparison between the observed and predicted patterns reveals that pores of ~14 vol.-% were generated in the resulting film,[23] which is smaller than that of the initial PMMA domains, 34 vol.-%. This large discrepancy may be attributed to several reasons:

i) UV exposure was insufficient to induce complete degradation of the PMMA block chains;[24] ii) the effective medium theory may describe composites possessing a lower contrast of the two dielectric constants, e.g., PMMA/PS: 2.22:2.53, better, but may not describe composites with higher contrast in dielectric constants, e.g., air/PS: 1:2.53 well;[22,25] iii) the number of guided modes in the s- and p- mode patterns was not enough to allow for precise evaluation; or iv) the beam spot did not probe the same area during the ex-situ experiment.

The porous templates were immersed in liquid media, a phosphate buffered saline (PBS) solution of pH 7.4, and ethanol (EtOH), in which most of the biological issues are explored. Filling of the pores with PBS followed by exchange with ethanol was detected as shifts of the resonance coupling modes to higher angles, illustrated in Figure 4.[26] The $\Delta\check{\imath}$ for TE_1 and TM_1 modes was 0.7° (from $\check{\imath} = 56.3°$ to $\check{\imath} = 57.0°$) and 1.8° (from $\check{\imath} = 48.8°$ to $\check{\imath} = 50.6°$), respectively. A large portion of this shift was induced by a change in the surroundings

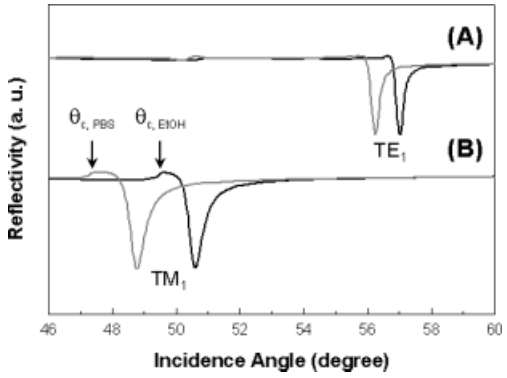

Figure 4. Waveguide mode patterns of the porous PS template filled with a pH 7.4 PBS solution (gray lines) and in ethanol (black lines) under s-polarization (A) and p-polarization (B), respectively. The critical angles under PBS and ethanol environments are marked by arrows.

above the template film (waveguide cladding), which was independently detected as a change in the critical angle from $\check{\imath}_{\text{c-PBS}}$ to $\check{\imath}_{\text{c-ethanol}}$, as marked by arrows in Figure 4B.[27] This change in cladding alone should produce shifts of TE_1 and TM_1 modes to 56.7 and 50.4°, respectively, as predicted by the Fresnel calculation. However, the final angles obtained in ethanol were 0.3 and 0.2°, higher than the changes due to cladding alone, for TE_1 and TM_1 modes, respectively. This verifies the exchange between the PBS solution and the optically denser ethanol in the pores. Here one also sees a stronger shift in p-polarization (Fig. 4B) than in s-polarization (Fig. 4A) when the process occurs inside the film. However, the insufficient number of guided modes did not allow for a precise calculation of the volume fraction of the pores filled by each liquid media.

In summary, thin films of BCPs with cylindrical microdomains oriented normal to the substrate surface were successfully coupled in the Kretschmann configuration, and their functions as optical waveguiding layers were demonstrated. Pore generation and exchange of pore materials inside the BCP films were monitored by shifts in the coupling mode angles. Similar experimental strategies applied to porous aluminum oxide templates demonstrated the subangstrom sensitivity of OWS for such processes.[27] Fresnel fitting to the observed waveguide patterns allowed for precise evaluation of the dielectric constants and film thicknesses independently. Based on the methodology established by this work, fabrication of one-dimensional nanostructures (e.g., nanowires or nanotubes) inside, or functionalization/adsorption on top of BCP templates can be investigated by static or in-situ kinetic-mode OWS. Moreover, organic waveguide materials with controlled periodic nanostructures and tunable dielectric constants can be developed for integrated optical devices. The porous BCP templates, which were shown to be stable in PBS solution and ethanol, also show promise for use as a versatile model platform by which interactions with biological substances (e.g., proteins or cells) can be probed. This work has discussed initial steps towards the use of BCP templates in applications such as optical sensing and biosensing.

Experimental

3-MPS was purchased from Lancaster Synthesis GmbH. Tetramethoxysilane (TMOS), Fluka GmbH, was used as the sol–gel precursor for the silicon dioxide layers. A typical solution for the precursors was composed of a mixture of 163 μL H_2O, 55 μL methanol, 81 μL 0.1 M HCl, and 20 μL TMOS. A commercial grade glass (n = 1.85; LaSFN9, Schott Glass GmbH) was used as a substrate onto which block copolymer thin films were fabricated.

PS-*b*-PMMA was prepared by using atom transfer radical polymerization as reported previously [28]. The volume fraction of the PMMA block was 0.30, and the weight-average molecular weight (M_w) was 55 500 with a polydispersity index of 1.19. Atatic PMMA homopolymers with $M_w = 23\,600$ were purchased from Polymer Sources, Inc. A hydroxy end-functionalized random copolymer of styrene and methyl methacrylate, denoted PS-*r*-PMMA, with a styrene fraction of 0.6, was synthesized in bulk via a TEMPO (2,2,6,6-tetramethylpiperidinyloxy) "living" free radical polymerization [19,20]. The molecular weight was determined to be $M_w = 9600$ with $M_w/M_n = 1.80$ (M_n = number-average molecular weight) determined by size exclusion chromatography.

AFM images were obtained using a Digital Instruments Dimension 3100 scanning force microscope in the tapping mode. Etched silicon tips on a cantilever (Nanoprobe) with spring constants ranging between 40.0 to 66.0 N m^{-1} were used.

A He–Ne laser with $\lambda = 632.8$ nm and 5 mW power was used to excite plasmon surface polaritons at the metal/dielectric interface. A polarizer for either s- or p-polarization was used for OWS. Both transverse electric (TE) and transverse magnetic (TM) modes (corresponding to s- and p-polarizations, respectively) were excited in the waveguide layers. To observe optical waveguide modes, reflectivity (R) was measured as a function of the incidence angle ($\check{\imath}$). The chopped beam was reflected off the gold-coated sample, which was mounted on a $\check{\imath}/2\check{\imath}$ goniometer, and the reflected intensity was then monitored by a photodiode that was read out by a lock-in amplifier.

Fresnel calculation was performed using the WINSPALL software (version 2.20) developed in the Max Planck Institute for Polymer Research in Mainz, Germany.

The block copolymer thin films were irradiated by deep UV light with a wavelength of 254 nm at a dose of 25 J cm^{-2} (XX-15S; UVP,

ADVANCED MATERIALS

Inc.) under vacuum for 30 min to selectively degrade the PMMA and crosslink PS, leaving behind the porous PS template.

Received: January 24, 2005
Final version: July 24, 2005
Published online: September 1, 2005

[1] I. W. Hamley, *The Physics of Block Copolymers*; Oxford University Press: New York, **1998**.
[2] G. H. Fredrickson, F. S. Bates, *Annu. Rev. Mater. Sci.* **1996**, *26*, 501.
[3] M. Lazzari, M. A. López-Quintela, *Adv. Mater.* **2003**, *15*, 1583.
[4] I. W. Hamley, *Angew. Chem. Int. Ed.* **2003**, *42*, 1692.
[5] R. E. Segalman, *Mater. Sci. Eng. Rev.* **2005**, *48*, 191.
[6] T. Thurn-Albrecht, J. Schotter, A. Kästle, N. Emley, T. Shibauchi, L. Krusin-Elbaum, K. Guarini, C. T. Black, M. T. Tuominen, T. P. Russell, *Science* **2000**, *290*, 2126.
[7] M. Park, C. K. Harrison, M. Chaikin, R. A. Register, D. H. Adamson, *Science* **1997**, *276*, 1407.
[8] A. M. Urbas, M. Maldovan, P. DeRege, E. L. Thomas, *Adv. Mater.* **2002**, *14*, 1850.
[9] H. Ma, A. K.-Y. Jen, L. R. Dalton, *Adv. Mater.* **2002**, *14*, 1339.
[10] J. T. Chen, E. L. Thomas, C. G. Zimba, J. F. Rabolt, *Macromolecules* **1995**, *28*, 5811.
[11] W. Knoll, *Annu. Rev. Phys. Chem.* **1998**, *49*, 569.
[12] W. Knoll, *MRS Bull.* **1991**, *16*, 29.
[13] J. D. Swalen, *J. Phys. Chem*. **1979**, *83*, 1438.
[14] E. Kretschmann, *Opt. Commun.* **1972**, *6*, 185.
[15] W. Knoll, in the *Handbook of Optical Properties Vol. II, Optical Properties of Small Particles, Interfaces and Surfaces*, (Eds.: R. E. Hummel, P. Wissmann) , CRC Press, Boca Raton, FL **1997**.
[16] U. Jeong, D. Y. Ryu, D. H. Kho, J. K. Kim, J. T. Goldbach, D. H. Kim, T. P. Russell, *Adv. Mater.* **2004**, *16*, 533.
[17] W. R. Thompson, M. Cai, M. Ho, J. E. Pemberton, *Langmuir* **1997**, *13*, 2291.
[18] J. W. Robertson, M. Cai, J. E. Pemberton, *Adv. Mater.* **2001**, *13*, 662.
[19] P. Mansky, T. P. Russell, C. J. Hawker, M. Pitsikalis, J. Mayes, *Macromolecules* **1997**, *30*, 6810.
[20] P. Mansky, Y. Liu, E. Huang, T. P. Russell, C. J. Hawker, *Science* **1997**, *275*, 1458.
[21] M. Maldovan, M. R. Bockstaller, E. L. Thomas, W. C. Carter, *Appl. Phys. B* **2003**, *76*, 877.
[22] C. G. Granqvist, O. Hunderi, *Phys. Rev. B* **1978**, *18*, 2897.
[23] A decrease of ε_D from 2.220 to 2.048 was calculated from comparison between the dielectric constant of the initial film ($\varepsilon_x = \varepsilon_y = 2.402$, $\varepsilon_z = 2.429$) and that of the porous template ($\varepsilon_x = \varepsilon_y = 2.377$, $\varepsilon_z = 2.385$). Then, the best fractional combination of air and PMMA was deduced to fit the effective constant of 2.048, using Equation 2.
[24] The film was subjected to the exposure conditions used to etch away PMMA domains in a thin PS-*b*-PMMA film of thickness ~L_0 (D. H. Kim, Z. Lin, H.-C. Kim, U. Jeong, T. P. Russell, *Adv. Mater.* **2003**, *15*, 811), which is about ten times thinner than the thickness used in this study.
[25] D. E. Aspnes, *Thin Solid Films* **1982**, *89*, 249.
[26] Note that the values of ε_{PBS} and ε_{EtOH} are 1.774 and 1.845, respectively.
[27] K. H. A. Lau, L.-S. Tan, K. Tamada, M. S. Sander, W. Knoll, *J. Phys. Chem. B.* **2004**, *108*, 10812.
[28] J. L. Wang, T. Grimaud, K. Matyjaszewski, *Macromolecules* **1997**, *30*, 6507.

Self-Organization of FePt Nanoparticles on Photochemically Modified Diblock Copolymer Templates**

By *Seth B. Darling*, *Nataliya A. Yufa*, *Amadou L. Cisse*, *Samuel D. Bader*, and *Steven J. Sibener**

Phase-segregated block copolymers have received significant attention in the last decade as enabling materials for future technologies.[1–6] Their value to nanotechnology derives from the expedient tunability of the size, shape, and periodicity of the self-assembled domains by means of manipulating molecular characteristics. Recently, the potential opportunities for block copolymer applications have been bolstered by new methods, which give fine control over long-range ordering of the microdomain structures.[4,5,7,9] Thin polymer films, by themselves, have limited device applications, but myriad functions can be addressed with hybrid hard/soft matter systems in which the organic layer is used as a scaffold for nanoscale organization of inorganic materials. Of specific interest is the interaction of surfactant-mediated colloidal nanoparticles and diblock copolymer films because the nanocrystal capping molecules can be tailored to exhibit preference for one of the polymer blocks.[10–13] This hierarchical approach to create ordered nanostructures removes the linear correlation of size and patterning time associated with traditional lithographic techniques by self-assembling the entire surface in parallel. Also, the spatial limits of lithography can be transcended and the approach can potentially be adapted to industrial-scale processing. An alternative approach to the colloidal nanocrystal methodology is to use spherical- or cy-

[*] Prof. S. J. Sibener, A. L. Cisse
James Franck Institute and Department of Chemistry
The University of Chicago
Chicago, IL 60637 (USA)
E-mail: s-sibener@uchicago.edu
Dr. S. B. Darling, Dr. S. D. Bader
Materials Science Division and Center for Nanoscale Materials
Argonne National Laboratory
Argonne, IL 60439 (USA)
N. A. Yufa
James Franck Institute and Department of Physics
The University of Chicago
Chicago, IL 60637 (USA)

[**] The authors thank Ward Lopes for useful discussions and A. C. Samia, J. Schleuter, and X. M. Lin for providing the FePt nanoparticles used in this study. The work was supported by the University of Chicago–Argonne National Laboratory Consortium for Nanoscience Research, the NSF-Materials Research Science and Engineering Center at The University of Chicago (NSF-DMR-0213745), and the AFOSR sponsored MURI Center for Materials Chemistry in the Space Environment. Work at Argonne is supported by the U.S. Department of Energy, Basic Energy Sciences-Materials Sciences, under Contract #W-31-109-ENG-38.

  DOI: 10.1002/adma.200500960